Est. 1984

ORIENTAL JOURNAL OF CHEMISTRY
An International Open Free Access, Peer Reviewed Research Journal

www.orientjchem.org

ISSN: 0970-020 X
CODEN: OJCHEG
2017, Vol. 33, No. (1):
Pg. 384-395

Preparation of L-Arginine-Modified Silica-Coated Magnetite Nanoparticles for Au(III) Adsorption

AMARIA AMARIA[1,2]*, NURYONO NURYONO[1] and SUYANTA SUYANTA[1]

[1]Department of Chemistry, Faculty of Mathematics and Natural Sciences, Universitas Gadjah Mada, Sekip Utara, Yogyakarta 55281, Indonesia.
[2]Department of Chemistry, Faculty of Mathematics and Natural Sciences, Universitas Negeri Surabaya, Jl. Ketintang, Surabaya 60231, Indonesia.
*Corresponding author E-mail: amaria@unesa.ac.id

http://dx.doi.org/10.13005/ojc/330146

(Received: December 04, 2016; Accepted: January 05, 2017)

ABSTRACT

L-arginine-modified silica-coated magnetite nanoparticles (Fe_3O_4/SiO_2-GPTMS-Arg) have been synthesized by sol-gel process for adsorption of Au(III) ion in aqueous solution. Modification of L-arginine on silica coated magnetite through a coupling agent of 3-glycidoxypropyl-trimethoxysilane (GPTMS) was performed in a various mole ratio of GPTMS:Arg 1:0; 1:1; 1:2 and 1:3. The products of Fe_3O_4/SiO_2-GPTMS-Arg were characterized with XRD, FTIR, EDX, TGA, and Kjeldahl methods. The results showed that based on characterization data Fe_3O_4/SiO_2-GPTMS-Arg has been successfully synthesized with the optimum mole ratio of 1:2. The optimum adsorption of Au(III) occurs at pH 3 and contact time of 60 min. The adsorption capacity followed Langmuir isotherm model was found 0.638 mmol.g^{-1} for the Fe_3O_4/SiO_2-GPTMS-Arg 1:2. Fe_3O_4/SiO_2-GPTMS-Arg nanoparticles show a potential adsorbent for an effective Au(III) ion removal.

Keywords: L-arginine, silica, magnetite, Au(III) ion adsorption.

INTRODUCTION

In the era of modern technology today, gold is not only used for fixing, but also for any application such as household appliances, electronics, cosmetics, biosensors and for the treatment of cancer cells[1,2]. In industrial processes and manufacturing various electronic equipment, stages of coating, washing, chemical and mechanical polishing are necessary. At the stage of washing or rinsing waste water containing precious metal and hazardous ions is often generated[3]. Even thought the waste water produced only containing metal ions in low concentrations, those may be harmful to human health and other living creatures. Therefore those are necessary to be managed and removed from the waste water.

A variety of techniques for wastewater treatment and separation of precious metal ions have been reported, such as chemical precipitation[4], ion exchange[5], adsorption[6,7], membrane filtration[8], and electrochemical[7,9]. Among of the above techniques, adsorption has been widely used since it is proven to be more effective and economical[10] because the design and operation are flexible. The adsorption is a reversible process so that the adsorbent can be regenerated through desorption process for reuse[11]. Efforts to develop the adsorbent containing selective functional groups have been conducted[12,13], but to recover precious metal ions and removal of heavy metal ion are still challenge. This is due to the capacity and selectivity towards targeted metal ions low and high cost [14]. Therefore, efforts to probe and develop a new adsorbent or method still continue.

The use of organic materials, such as organic polymers, cellulose, algae, and yeast biomass as adsorbent has a weakness, such as swelling, very sensitive to chemicals and lower its mechanical stability. In other hands, support inorganic solids, such as clay, zeolite, metal oxides and silica are preferable due to relatively resistant in term of physicochemistry and good selectivity. Silica gel has attracted the attention of researchers, because of high chemical and mechanical stabilities and low swelling[15]. In addition, the silica containing a lot of silanol groups on the surface makes easy to be modified with the organic functional group.

Modification of silica gel with amine groups has been reported to be highly efficient in removing of Cu(II), Ni(II), Pb(II), Cd(II), Zn(II) and Hg(II) ions in aqueous medium[16,17]. Aminoguanidine groups have been used as a modifier of adsorbent from the tannin extract of persimmon for recovery of Au(III) ion in acidic media[18]. Therefore, ligands with amine functional groups are very effective to adsorb precious metal ions[19]. Modification of the silica gel with the active site of mercapto (-SH) and an amine (NH_2) has been reported by Nuryono et al.[20] for Au(III) ion adsorption. The hybrid of amino-silica adsorbed the Au(III) ion in similar amount (98.77%) to that of mercapto-silica (96.67%) at the pH 4. In that condition, the amine groups of the amino-silica hybrid surface are protonated to form cationic groups $-NH_3^+$ and interact with anionic species of Au(III) ion, $AuCl_4^-$. The interaction between Au(III) ion with amino-silica hybrid might happen through ionic interactions. While the mercapto-silica hybrid, the S atoms donate the electron pair to Au(III) ions to form complexes using covalent interactions.

Nowadays, magnetic separation is considered as an effective method for the recovery precious metals and removal of heavy metal ions. Magnetite nanoparticles (Fe_3O_4) modified with functional groups such as dendrimer[21], dimethylamine[22], dimercaptosuccinic acid[23], and 3-aminopropyltrietoksisilan[24] has been tested to be capable of removing heavy metal ions due to the high adsorption ability, time is short and separation of the adsorbent from the solution is easy because it uses an external magnetic field. The active site which contains a nitrogen or a sulfur atom is selectively high for the precious metal ion according to the hard soft acid base (HSAB) theory[25]. The magnetite nanoparticles which modified by thiourea ($SC(NH_2)_2$)[26] have been reported to be capable of separating and recovering precious metal ions from acid solution.

L-arginine molecules have a flexible chain of guanidine groups with pKa of 12.5.[27] Guanidine ($-NHCNHNH_2$) groups with a positive charge in acidic or neutral conditions leads to adsorb $AuCl_4^-$ anion from species of Au(III) ion[18]. In this research, we have prepared L-arginine modified silica coated on magnetite nanoparticles surface using a linker of 3-glycidoxypropyl-trimethoxysilane (GPTMS) in the sol-gel system. The effect of a mole ratio of L-arginine to GPTMS on the chemical stability, the content of nitrogen and the adsorption properties for adsorption of Au(III) ions in aqueous solution has been evaluated.

MATERIALS AND METHODS

In this study, we used chemicals such as iron (II)/(III) oxide, 3-glycidoxypropyl-trimethoxysilane (GPTMS) (≥ 98%) from Sigma-Aldrich. Sodium silicate (25-27%), L-arginine powder, ethanol absolute (99.5%), HCl 37%, NaOH, HNO_3 65%, thiourea, gold standard solution were purchased from Merck used without previous treatment. Precious metal of gold was purchased from PT. Aneka Tambang.

Preparation of L-Arginine-Modified Silica-Coated Magnetite Nanoparticles (Fe_3O_4/SiO_2-GPTMS-Arg)

In a beaker polyethylene, magnetite 0.4 g was added with 10 mL of distilled water and sonicated for 5 minutes. After that, the suspension was added 12 mL of 2.8 M Na_2SiO_3 solution and sonicated. After the suspension stirred mechanically for 30 minutes, it was added 1.13 mL of GPTMS and stirred it about 30 minutes. Furthermore, the suspension was added with 5 mmol L-arginine in order the mole ratio of GPTMS to L-arginine 1:1, stirred for 60 minutes and 2 M HCl added dropwise until pH 7 and formed a gel. After the gel left in one night, gel washed with aqua mineral and flushed with ethanol three times, and dried at 65°C in the oven until its weight of constant (See Fig 1). Analogue work was conducted varying the mole ratio of GPTMS to L-arginine according to Table 1.

Characterization

The functional groups in samples were identified with FTIR spectrophotometer (Shimadzu FTIR 8400S) with KBr pellet technique in wave number 400-4000 cm^{-1}. Powder XRD pattern of samples was compiled on Bruker D8 Advance 206276 (Source used radiation of Cu-Kα (λ 0.154 nm) on 40 kV voltage and 30 mA current. X-ray diffraction patterns were scanned at a 2è range of 3-80° in scan speed 5°/minutes. The nitrogen content of samples was counted with energy dispersive X-ray (EDX Carl Zeiss 9 EVO MA 10 series 1454) and Kjeldahl method. TGA was carried out on Mettler Toledo with a rate of heating 20°C per minute, at temperature 40-800°C. Absorption atomic spectrophotometer Analyst 100 Perkin Elmer apparatus was used to define the content of metal ion in solution. Niobium magnet was used for the magnetic separation. The measurement of the pH solution was conducted with a pH meter (pH/ion 510 Eutech Oakton).

The chemical stability was tested by mixing 25 mg of sample with 25 mL HCl solution 1 M and shaking for 3 hours. After that, it was left overnight at a room temperature. The filtrate was divided from the mixture by an external magnetic force and dissolved iron was determined by atomic absorption spectroscopy method[28,29].

Adsorption of Au(III)

Adsorption of Au(III) on Fe_3O_4/SiO_2-GPTMS-Arg was conducted by the effect of pH, adsorption time and concentration of Au(III) ions. Adsorbent 10 mg was added to 10 mL of Au(III) solution in a batch system of a polyethylene bottle at a room temperature (302 K). The mixture was shaken at 350 rpm for certain time and the adsorbent was separated with an external magnet. The concentration of Au(III) ion not adsorbed in the supernatant was measured by Atomic Absorption Spectrophotometer (AAS). A number of Au(III) ions adsorbed was calculated by the difference between the initial and final concentration of Au(III) in the supernatant using Eq. (1)

$$q = \frac{(C_0 - C_e)V}{W} \quad ...(1)$$

q is Au(III) ions adsorbed (mmol.g^{-1}); C_0 and C_e are initial and final concentrations of Au(III) (mmol.L^{-1}), respectively. V is volume (L) of the Au(III) solution and W is the adsorbent mass (g).

The pH of medium was controlled by 0.1 M HCl and/or 0.1 M NaOH solution to reach 1-5, the effect of concentration of Au(III) ion was carried on 25-250 mg L^{-1} and the variation of contact time was observed at the range of 5-180 minutes. The models of Langmuir and Freundlich isotherm were applied to evaluate data of the effects of initial concentration and the models of some kinetics reaction are used to verify the appropriate adsorption rate constant.

The experiment of desorption was conducted by using thiourea solution in 1 M HCl-HNO_3. The firstly, 200 mg of adsorbent was added with 50 mL 100 mg.L^{-1} Au(III) at optimum pH for 60 minutes. After the mixture was shaken and separated with a magnet, the supernatant was analyzed by AAS to decide the content of Au(III) not absorbed. The adsorbent loaded with Au(III) was washed by aquamineral and dried at 65°C to get the weight of constant and stored in a desiccator overnight before desorption process. The adsorbent loaded with Au(III) was added with 10 mL of H_2O, and then was shaken for 10 min and supernatant was separated with an external magnet. The supernatant was analyzed by AAS to decide the content of Au(III) that leached with H_2O. The adsorbent-loaded was added with 10 mL of 0.5 M thiourea solution in 1M HCl. Then

the mixture was shaken for 8 h and separated with a magnet, and the Au(III) ion released was measured its concentration. The desorption was repeated three times using the same eluent. Desorption data of Au(III) was calculated with Eq 2[30]:

$$\%Desorption\ efficiency = \frac{released\ gold\ (mg)}{initialy\ adsorbed gold (mg)} x100 \quad ...(2)$$

RESULTS AND DISCUSSION

Characteristic of Fe_3O_4/SiO_2-GPTMS-Arg Functional groups

The FT-IR spectra of silica-coated magnetite nanoparticles with and without L-arginine modification are showed in Fig 2. All spectra have a peak at 568.96 cm^{-1}. The peak is ascribed to Fe-O mode of magnetite[31]. Peaks 3446.56 cm^{-1} and 1645.17 cm^{-1} are associated the O-H stretching and bending vibration, respectively (Fig 2a). The characteristic peak of silica is observed at around of 1100 cm^{-1} related to the Si-O(Si-O-Si) asymmetric stretching vibration[32]. In all spectra, the peak at 796.55 cm^{-1} is observed, assigned to symmetric stretching of siloxane Si-O(Si-O-Si), while the band around 460.96 cm^{-1} corresponds to the Si-O-Si or O-Si-O bending modes[33]. This suggests that silica has been coated on the magnetite surface[34]. From Fig 2(b-d) can be seen peaks at 3415.70, 3443.06 and 3411.84 cm^{-1} ascribing the presence of amino groups. Those peaks are apparent broader than that of Fig 2a due to overlapping with O-H stretching vibration.

Peak around 2939.31 cm^{-1} is appointed to the stretching vibration of C-H asymmetric[32], from GPTMS and L-arginine. The peak at 1645.17 cm^{-1} (Fig 2a) is related the O-H (Si-OH) bending vibration (due to condensation of GPTMS), while the peak at 1654.81, 1662.52, and 1656.74 cm^{-1} (Fig 2b-d) are related to the N-H bending vibration[18,35]. It indicates that the coupling agent of GPTMS and modifier of L-arginine have been modified on silica-coated magnetite nanoparticles surface.

Crystalline Structure

The X-ray diffraction pattern of the L-arginine modified silica coating on magnetite nanoparticles surface synthesized with various mole ratios of GPTMS to L-arginine are presented in Fig. 3. The observation of X-ray diffraction pattern for four samples seems characteristic peaks of magnetite confirmed by JCPDS 19-0629 with the index field (220), (311), (400), (511) and (440)[36], and hence it denote that the cubic crystal phase of magnetite is stand after coating with L-arginine-modified silica[37]. The presence of SiO_2 amorphous phase is showed by specific 2θ at 22 degrees[38] (Fig. 3b, c, d, and e) according to JCPDS No. 46-1045.

Chemical stability

Magnetite powder is readily dissolved in acidic solution[39]. Silica coating may stabilize magnetite from an acidic medium[34,39,40]. In this work, the magnetite nanoparticles were coated with silica and added a modifier of L-arginine. The samples of Fe_3O_4/SiO_2-GPTMS-Arg obtained were mixed with hydrochloric acid 1 M for 1 day. Iron leached from the sample was determined with AAS. The result showed that the acid solution leached iron from the coated magnetite samples in a range of 0.235-0.344 mmol g^{-1}. It is much lower than the amount of iron leached from uncoated magnetite (1.09 mmol g^{-1}).

The content of nitrogen element

L-arginine as a modifier to the silica coated magnetite contains amine groups which may react well with Au(III) in solution. Based on the FTIR spectra in Fig. 2 seem that coated magnetite contains amine group -NH from L-arginine. In addition, we also confirmed the presence of nitrogen element from L-arginine using the EDX and Kjeldahl methods[41] and the result is expressed in Table 4. The content of nitrogen in sample synthesized with a mole ratio of GPTMS to Arginine 1:2 and 1: 3 analyzed with EDX and Kjeldahl methods are relatively similar and higher than in sample synthesized with the ratio 1:1. However, the content of nitrogen based on the theoretical calculation is much greater than result from the experiment. This difference occurs probably since not all arginines are bonded on the surface. The presence of nitrogen in all samples supports the success of modification of arginine on silica coated magnetite.

Thermogravimetric Analysis

Thermogravimetric analysis (TGA) was conducted on four samples of magnetite coated with silica-arginine at temperatures from 40-800°C, with the heating rate of 20°C per minute. Fig. 4 shows that

there are four stages of weight loss in the TGA curve. The first stage, degradation occurs at a temperature of 40-100°C, the second stage of 100-250°C, the third stage of 250-500°C, and the fourth stage of 500-800°C. In Fig. 4 is observed that all four samples of coated magnetite lost the weight at a temperature of 40-100 °C (<100 °C). The weight loss is related to the removal of water molecules adsorbed physically, which removal of water molecules is continued at the temperature of 100-220°C [42,43]. Fig. 4 shows that the weight loss in the second stage at that temperature range (100-250°C), for Fe_3O_4/SiO_2-GPTMS-Arg 1:0, 1:1, 1:2, 1:3 is 3.279; 3.384; 4.306 and 4.707%, respectively.

At the temperature range of 250-500°C, TGA curves of Fe_3O_4/SiO_2-GPTMS-Arg 1:0 the weight loss is 9.208%. The weight loss is linked to the decay of the organic part of a silica network, as reported Shajesh *et al.*[43]. Another reason of the weight loss is a dehydration and dehydroxylation reaction of silanol (vicinal, geminal, and combinations) in the silica[42,44]. Meanwhile, Fe_3O_4/SiO_2-GPTMS-Arg 1:1, 1:2, and 1:3 at the temperature range of 250-500°C loosed the weight of 7.570, 18.549, and 17.577 %, respectively. In that temperature, the decomposition of organic parts[43,45], including L-arginine bound to the silica network produces CO and CH_4. At higher temperature than 500°C NH_3 is released. At a temperature range of 250-500 °C show that the percentage of the weight loss is higher for L-arginine-modified silica-coated magnetite sample prepared with greater mole ratio. This phenomenon can be explained that smaller size nanoparticles have the larger surface area so that it can bind arginine on the surface in larger number, and the percentage of weight loss is greater[46,47].

Table 1: Mole ratio of GPTMS to L-arginine on preparation of the L-arginine modified silica-coated magnetite nanoparticles

mmol GPTMS	mmol L-arginine	Mole ratio GPTMS/ L-arginine	Sample Label
5	0	1:0	Fe_3O_4/SiO_2-GPTMS-Arg 1:0
5	5	1:1	Fe_3O_4/SiO_2-GPTMS-Arg 1:1
5	10	1:2	Fe_3O_4/SiO_2-GPTMS-Arg 1:2
5	15	1:3	Fe_3O_4/SiO_2-GPTMS-Arg 1:3

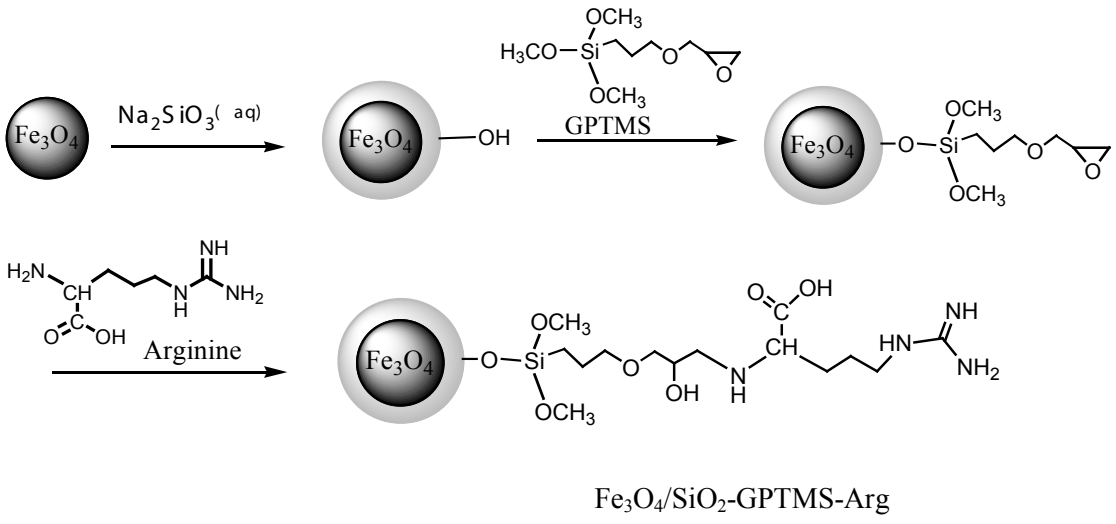

Fig.1: Predicted reaction route of coating L-arginine modified silica on magnetite nanoparticles

At a temperature range of 500-800°C (in the fourth stage), the weight loss is related to the silanol dehydroxylation, especially silanol in geminal position[42]. Thermal decomposition of all sample at this temperature are decreasing, this shows that all the decomposition stopped. In addition, at temperature 500°C, the magnetite is changed into hematite[48].

Adsorption properties

Effect of medium pH on the Au(III) ion adsorption

The experimental result to study the effect of pH on is presented in Fig. 5 showing that for all investigated adsorbents adsorption of Au(III) reaches optimum at pH 3. In the highly acidic condition (at pH 1-2), the adsorption is very low and

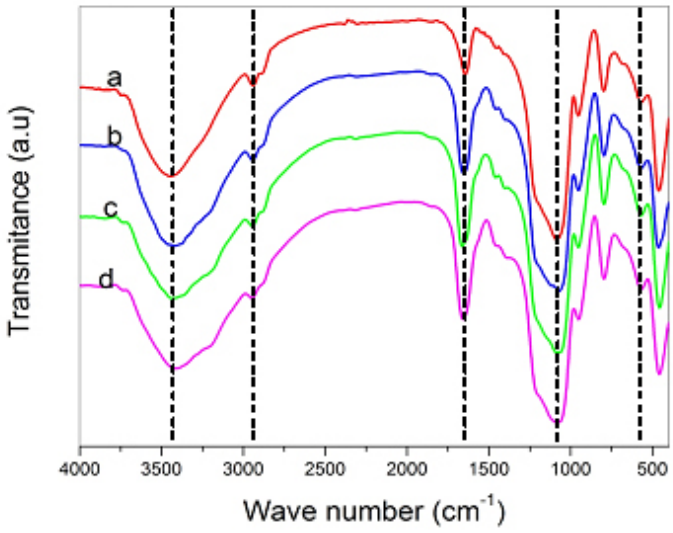

Fig. 2: FTIR spectra of Fe_3O_4/SiO_2/GPTMS-Arg 1:0 (a), Fe_3O_4/SiO_2-GPTMS-Arg 1:1 (b), Fe_3O_4/SiO_2-GPTMS-Arg 1:2 (c), and Fe_3O_4/SiO_2-GPTMS-Arg 1:3 (d)

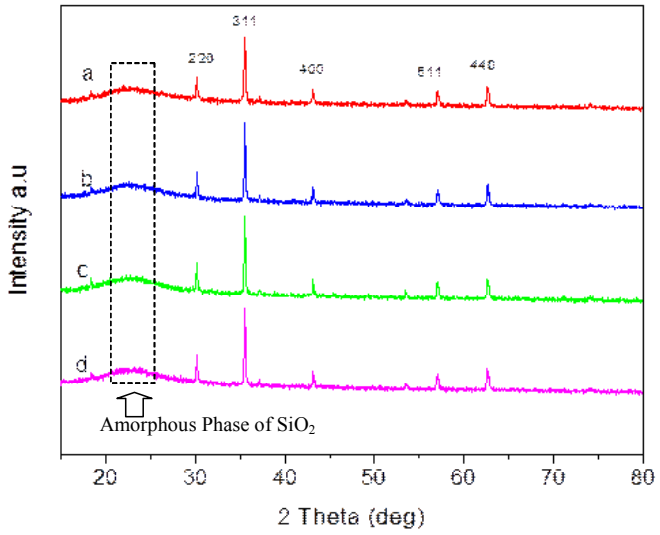

Fig. 3: XRD patterns of Fe_3O_4/SiO_2-GPTMS-Arg 1:0 (a) Fe_3O_4/SiO_2-GPTMS-Arg1:1 (b), Fe_3O_4/SiO_2-GPTMS-Arg1:2 (c), and Fe_3O_4/SiO_2-GPTMS-Arg 1:3 (d)

at higher pH (above 3), the adsorption decreases. Adsorbents Fe_3O_4/SiO_2-GPTMS-Arg 1:1, 1:2, and 1:3 show relatively similar adsorption capability (61.95, 67.45, and 66.88 mg g^{-1}, respectively). Fe_3O_4/SiO_2-GPTMS-Arg 1:0 gives very low adsorption capability. It is associated with the active site in the magnetic adsorbent surface, without L-arginine, the probable active site playing a role in adsorption is only -OH of GPTMS. Au(III) in solution at pH 2-3 is dominant as a stable complex ion $[AuCl_4]^-$and at increased pH, chloride ion in the complex $[AuCl_4]^-$ is replaced by OH^- ions. At a pH of 4-9 in $[AuCl_3OH]^-$ $[AuCl_2OH_2]^-[AuClOH_3]^-$ are formed and at pH higher than 9 the $[AuOH_4]^-$ form dominates[49]. In the acidic condition amino groups (NH_2) of arginine on silica-coated magnetite nanoparticles surface undergo protonation to generate positively charged groups ($-NH_3^+$). Those groups may interacts electrostatically with $AuCl_4^-$, a species of Au(III) in acidity. As seen in Fig. 5 the adsorption of Au(III) at pH 3 is observed maximum. The interaction between the surface of Fe_3O_4/SiO_2-GPTMS-Arg and Au(III) metal ions in acidic conditions is illustrated hypothetically in Fig. 6.

Adsorption isotherm of Au(III)

The adsorption isotherms of Au(III) on four magnetic adsorbents were tested with the effect

Table 4: The content of nitrogen in L-arginine modified silica-coated magnetite nanoparticles based on measurements of EDX, Kjeldahl method, and the theoretical calculation

Method	wt% N		
	Fe_3O_4/SiO_2-GPTMS-Arg 1:1	Fe_3O_4/SiO_2-GPTMS-Arg 1:2	Fe_3O_4/SiO_2-GPTMS-Arg 1:3
EDX	3.28	4.86	4.07
Kjeldahl	2.478	3.610	3.958
Theoretical calculation	6.189	10.386	13.421

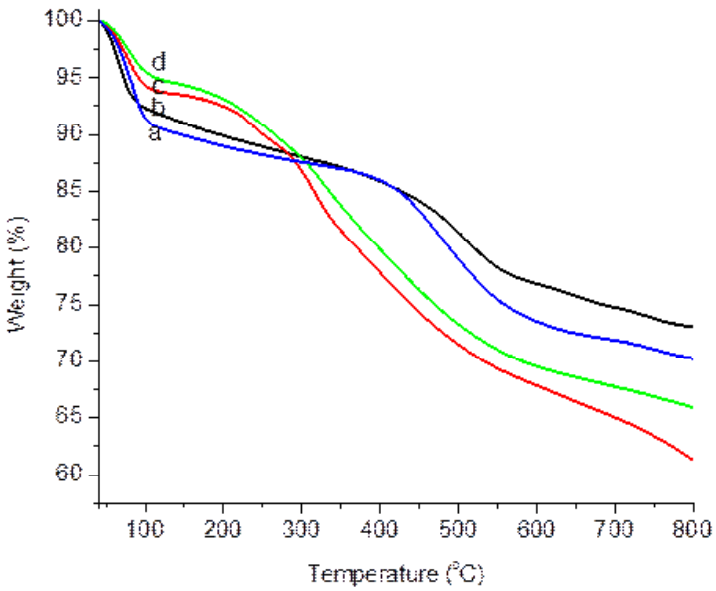

Fig. 4: Thermogravimetry analysis curve of Fe_3O_4/SiO_2/GPTMS-Arg 1:0 (a), Fe_3O_4/SiO_2-GPTMS-Arg 1:1 (b), Fe_3O_4/SiO_2-GPTMS-Arg 1:2(c), and Fe_3O_4/SiO_2-GPTMS-Arg 1:3(d)

of initial concentrations of Au(III) (25-250 mg/L) at pH 3. The adsorption experimental data were evaluated by Langmuir and Freundlich isotherm models[34,50] expressed in mathematical equation (Eq. 3 and 4).

$$\frac{C_e}{q_e} = \frac{1}{K_L q_m} + \frac{1}{q_m} C_e \quad ...(3)$$

$$\log q_e = \log K_F + \frac{\log C_e}{n} \quad ...(4)$$

where q_e and C_e are the amount Au(III) adsorbed and concentration of Au(III) at equilibrium,

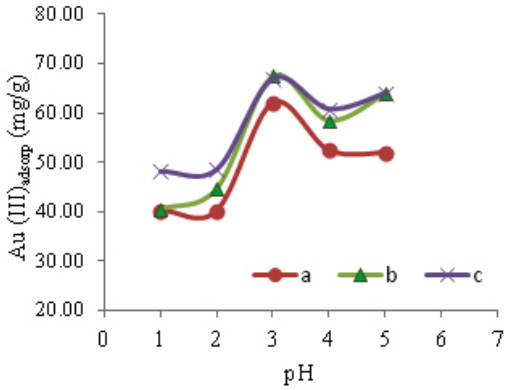

Fig. 5: Effect of pH on Au(III) ion adsorption by Fe_3O_4/SiO_2-GPTMS-Arg 1:1(a), Fe_3O_4/SiO_2-GPTMS-Arg 1:2 (b), and Fe_3O_4/SiO_2-GPTMS-Arg 1:3 (c)

q_m is adsorption capacity and K_L is the constant of Langmuir relating to the binding sites affinity. The value of q_m obtained from slope and K_L found from the intercept of a plot of C_e/q_e vs C_e. K_F. The constant of Freundlich is related to the adsorption capacity and n is Freundlich exponent linked to the intensity of adsorption. The values of K_F and n are obtained from slope and intercept of plot log q_e vs log C_e. The adsorption process according to Langmuir isotherm is assumed as monolayer and occurs on the sites of the homogenous surface. While the Freundlich isotherm assumed that the adsorption is held on the sites of the heterogeneous surface. The adsorption data of Au(III) on Fe_3O_4/SiO_2-GPTMS-Arg 1:0-1:3 are shown in Fig 7 and Table 5 presents the Langmuir and Freundlich isotherm constants for adsorption of Au(III) on Fe_3O_4/SiO_2-GPTMS-Arg 1:0-1:3. The linear coefficient (R^2) values for Langmuir isotherm models, in general, are higher than 0.99. This indicates that the Langmuir isotherm fits for the experimental data of Au(III) adsorption.

From Table 5 can be seen that the value of the adsorption capacity of Fe_3O_4/SiO_2-GPTMS-Arg increases with the mole number of L-arginine added, namely 0.209; 0.544; 0.638; 0.654 mmol/g, which correspond to the nitrogen content. This indicates that functional group participates in the adsorption is $-NH_3^+$. The adsorbent without L-arginine (Fe_3O_4/SiO_2-GPTMS-Arg 1:0) gives lowest adsorption capacity and the adsorbents containing L-arginine show capacity 1.87-3.13 times higher. The value of $\Delta G°$ (Table 5) are higher than 21 kJ/mol[51] indicating the involvement of chemical interaction, as illustrated in hypothetic reaction (Fig 6).

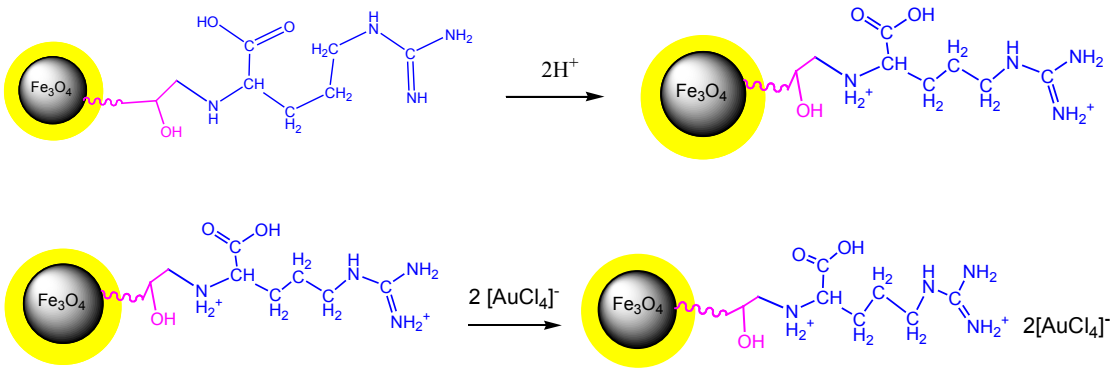

Fig. 6: Hypothetic reaction on the formation of ionic bonds between Fe_3O_4/SiO_2-GPTMS-Arg with Au(III) ion in aqueous solution

Adsorption kinetics

Study on the kinetics of Au(III) adsorption was conducted by interacting with 50 mg L^{-1} Au(III) solution at various contact times (5-180 min), pH 3 and room temperature (302 K). The adsorption data is presented in Fig. 8. It is observed that in the first five minutes adsorption occurs rapidly, followed by slow inclining and lastly reached equilibrium after 60 minutes. It was associated with a lot number of sites on the coated magnetite adsorbent surface available for Au(III) in the early reaction and finalized with equilibrium after saturation.

The reaction kinetics models of pseudo-first-order and pseudo-second-order were applied to evaluate the adsorption of Au (III) on the adsorbents, two common models for adsorption of metal ions on a solid adsorbent. The reaction kinetics models of pseudo-first-order and pseudo-second-order are stated in Eq (5) and (6), respectively[52,53].

$$\ln(q_e - q_t) = \ln(q_e) - k_1 t \quad ...(5)$$

$$\frac{t}{q_t} = \frac{1}{k_2 q_e^{\,2}} + \frac{1}{q_e} t \quad ...(6)$$

q_e and q_t are the amounts of adsorbed metal ion at equilibrium and anytime, respectively (mmol. g^{-1}), and k_1 (min^{-1}) and k_2 ($g.mmol^{-1}.min^{-1}$) are the rate constants of pseudo-first-order and pseudo-second-order. The rate constants can be determined from the linear curve plot of (ln q_e - q_t) against t and t/q_t against t to pseudo-first order and pseudo-second

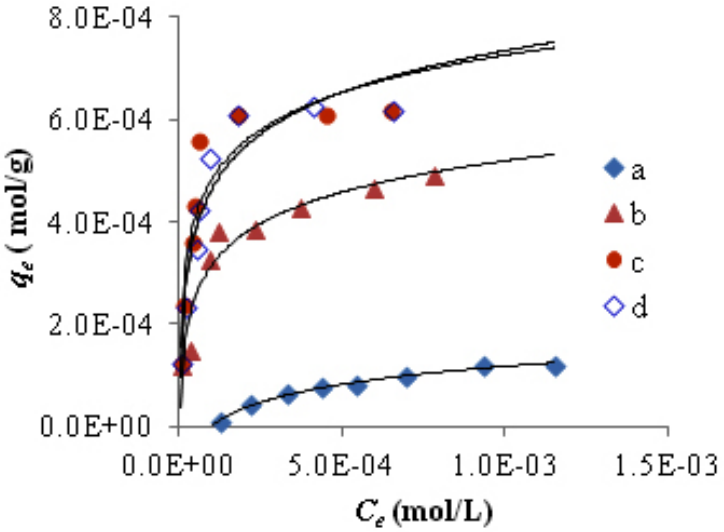

Fig. 7: Adsorption isotherm of Au(III) on Fe_3O_4/SiO_2-GPTMS-Arg 1:0 (a), Fe_3O_4/SiO_2-GPTMS-Arg 1:1 (b), Fe_3O_4/SiO_2-GPTMS-Arg 1:2 (c), Fe_3O_4/SiO_2-GPTMS-Arg 1:3 (d)

Table 5: Adsorption isotherm parameters of Au(III) on Fe_3O_4/SiO_2-GPTMS-Arg

Adsorbent	Langmuir				Freundlich		
	q_{max} (mmol/g)	K (10^{-3}) (L.mol^{-1})	ΔG° (KJ. mol^{-1})	R^2	K_F (10^{-2}) (mol/ g^{-1})	n	R^2
Fe_3O_4/SiO_2/ GPTMS-Arg 1:0	0.209	1.264	17.933	0.968	22.0	0.94	0.831
Fe_3O_4/SiO_2/ GPTMS-Arg 1:1	0.544	17.467	24.525	0.995	0.61	2.98	0.907
Fe_3O_4/SiO_2/ GPTMS-Arg 1:2	0.638	48.042	27.066	0.999	0.78	3.21	0.827
Fe_3O_4/SiO_2/ GPTMS-Arg 1:3	0.654	33.671	26.174	0.997	1.00	2.87	0.890

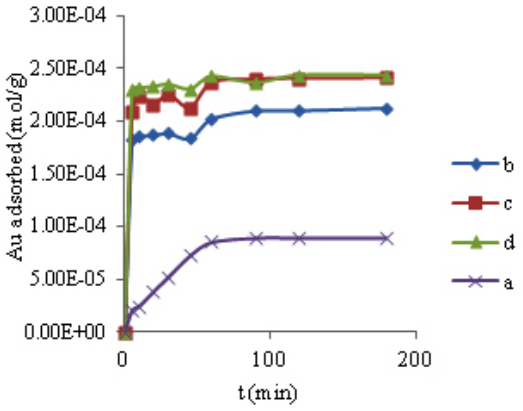

Fig. 8: Effect of time on Au(III) ion adsorption on Fe_3O_4/SiO_2-GPTMS-Arg 1:0 (a), Fe_3O_4/SiO_2-GPTMS-Arg 1:1(b), Fe_3O_4/SiO_2-GPTMS-Arg 1:2 (c), Fe_3O_4/SiO_2-GPTMS-Arg 1:3 (d)

order reactions, respectively. The result of calculation is presented in Table 6, showing that the adsorption kinetics model of pseudo-second order is more suitable with the higher linear coefficient (R^2) value (0.999) than pseudo-first-order one. This shows that the adsorption system involves the exchange of electrons between the magnetic adsorbent and Au(III) ion in aqueous solution[37,53].

Desorption

The Au(III) ion adsorbed on Fe_3O_4/SiO_2-GPTMS-Arg was recovered by sequence desorption experiments. Desorption of precious metals by using a thiourea solution, HCl, thiourea-HCl, HNO_3, thiourea-HNO_3 has been reported by previous researchers[22,26,30,54,55]. In this work, desorption of Au(III) adsorbed on Fe_3O_4/SiO_2-GPTMS-Arg 1:2 (25.068 mg/g) was carried out within the different

Table 6: Adsorption rate constant of Au(III) on adsorbents based on the kinetics models of pseudo-first and pseudo-second order

Sample	Kinetics model			
	Pseudo-first order		Pseudo-second order	
	k (min^{-1})	R^2	k ($g.mmol^{-1}.min^{-1}$)	R^2
Fe_3O_4/SiO_2-GPTMS-Arg 1:0	0.0708	0.9665	0.3701	0.9830
Fe_3O_4/SiO_2-GPTMS-Arg 1:1	0.0255	0.8811	1.3969	0.9988
Fe_3O_4/SiO_2-GPTMS-Arg 1:2	0.0380	0.9792	1.7721	0.9991
Fe_3O_4/SiO_2-GPTMS-Arg 1:3	0.0352	0.8711	3.5172	0.9997

Table 7: The desorption data of Au(III) loaded on Fe_3O_4/SiO_2-GPTMS-Arg 1:2 with different eluents

Desorber eluent	Fraction/Eluent	Au(III) desorbed (%)	Desorption Total (%)
0.5 M Thiourea-1 M HCl	10 mL Aquademineral	0.5231	60.8431
	10 mL Thiourea - HCl	57.8411	
	10 mL Thiourea - HCl	2.4789	
	10 mL Thiourea - HCl	0	
1 M Thiourea-0.5 M HCl	10 mL Aquademineral	0	75.2997
	10 mL Thiourea - HCl	54.7049	
	10 mL Thiourea - HCl	20.4661	
	10 mL Thiourea - HCl	0.1287	
0.5 M Thiourea-1M HCl-1M HNO_3 (3:1)	10 ml Aquademineral	0	64.3061
	10 mL Thiourea - HCl - HNO_3	58.4736	
	10 mL Thiourea - HCl - HNO_3	5.6993	
	10 mL Thiourea - HCl - HNO_3	0.1332	

composition of eluent at a room temperature as presented in Table 7. Each fraction (10 mL) of desorption, the concentration of Au(III) desorbed was determined with AAS. As shown in Table 7, desorption using 1 M thiourea-0.5 M HCl gives the highest desorption percentage (75.2997%). However, this result has not satisfied yet and the investigation is still going on to reach 100 % of recovery.

CONCLUSION

In conclusion, L-arginine-modified silica-coated magnetite nanoparticles (Fe_3O_4/SiO_2-GPTMS-Arg) have been successfully synthesized using 3-glycidoxypropyl trimethoxysilane as the coupling agent via a sol-gel process with the optimum mole ratio of GPTMS to arginine of 1:2. Adsorption of Au(III) on Fe_3O_4/SiO_2-GPTMS-Arg 1:2 occurred optimally at pH 3, followed the model of pseudo-second-order with a rate constant of 1.77 g. $mmol^{-1}.min^{-1}$ and fitted to the model of Langmuir isotherm with the capacity of 0.64 $mmol.g^{-1}$. The further investigation to find the best desorption technique in which Au(III) may be leached from adsorbent 100 % is still going on, and it is expected that magnetic material produced may be useful for recovery of precious metals from both industrial waste water and precious metal mining samples.

ACKNOWLEDGEMENT

We would like to give the highest gratitude to the Ministry of Research, Technology and Higher Education of the Republic of Indonesia through the Research Grant *Disertasi Doktor* 2016 and Postgraduate Scholarship for the financial support.

REFERENCES

1. Widmer, R.; Oswald-Krapf, H.; Sinha-Khetriwal, D.; Schnellmann, M.; Böni, H. *Environ. Impact Assess. Rev.* **2005**, *25* (5 SPEC. ISS.), 436–458.
2. Guix, M.; Carbonell, C.; Comenge, J.; García–Fernández, L.; Alarcón, A.; Casals, E. *Contrib. to Sci.* **2008**, *4* (2), 213–217.
3. Cui, J.; Zhang, L. *J. Hazard. Mater.* **2008**, *158* (2), 228–256.
4. Fu, F.; Wang, Q. *J. Environ. Manage.* **2011**, *92* (3), 407–418.
5. Dabrowski, A.; Hubicki, Z.; Podkoscielny, A.; Robens, E. *Chemosphere* **2004**, *56*, 91–106.
6. Lopes, C. B., Lito, P. F., Cardoso, S. P., Pereira, E., Duarte, A. C., and S. C. M. *Ion Exchange Technology II*; Inamuddin and M. Luqman, Ed.; Springer Science+Business Media B.V, 2012; Vol. 10.
7. Cornell, R. M.; Schwertmann, U. *Introduction to the Iron Oxides*, 2nd Editio.; WILEY-VCH Verlag GmbH & Co. KGaA, Weinheim All: Darmstadt, 2004.
8. Camarillo, R.; Llanos, J. *Sep. Purif. Technol.* **2010**, *70*, 320–328.
9. Kurniawan, T. A.; Chan, G. Y.; Lo, W.-H.; Babel, S. *Chem. Eng. J.* **2006**, *118* (1), 83–98.
10. Ekmekyapar, F.; Aslan, A.; Bayhan, Y. K.; Cakici, A. *J. Hazard. Mater.* **2006**, *137* (1), 293–298.
11. Pan, B.; Pan, B.; Zhang, W.; Lv, L.; Zhang, Q.; Zheng, S. *Chem. Eng. J.* **2009**, *151* (1–3), 19–29.
12. Ngah, W. W.; Fatinathan, S. *J. Environ. Manage.* **2010**, *91* (4), 958–969.
13. Liu, C.-C.; Wang, M.-K.; Chiou, C.-S.; Li, Y.-S.; Lin, Y.-A.; Huang, S.-S. *Ind. Eng. Chem. Res.* **2006**, *45* (26), 8891–8899.
14. Hubicki, Z.; Wo\lowicz, A. *Hydrometallurgy* **2009**, *96* (1), 159–165.
15. Jal, P. K., Patel, S., Mishra, B. K. *Talanta* **2004**, *62* (5), 1005–1028.
16. Aguado, J.; Arsuaga, J. M.; Arencibia, A.; Lindo, M.; Gascón, V. *J. Hazard. Mater.* **2009**, *163* (1), 213–221.
17. Radi, S.; Basbas, N.; Tighadouini, S.; Bacquet, M.; Degoutin, S.; Cazier, F. *Prog. Nanotechnol. Nanomater.* **2013**, *2*, 108–116.
18. Gurung, M.; Adhikari, B. B.; Morisada, S.; Kawakita, H.; Ohto, K.; Inoue, K.; Alam, S. *Bioresour. Technol.* **2013**, *129*, 108–117.
19. Adhikari, C. R.; Parajuli, D.; Inoue, K.; Ohto, K.; Kawakita, H.; Harada, H. *New J. Chem.* **2008**, *32* (9), 1634–1641.

20. Nuryono, N.; Indriyanti, N. .; Manuhuntu, J. .; Narsito; Tanaka.S; Rosiati, N.; Rusdiarso, B.; Sakti, S. C.; Tanaka, S. *Malaysian J. Anal. Sci.* **2013**, *3* (1), 244–254.
21. Chou, C.-M.; Lien, H.-L. *J. Nanoparticle Res.* **2011**, *13* (5), 2099–2107.
22. Zhou, L.; Xu, J.; Liang, X.; Liu, Z. *J. Hazard. Mater.* **2010**, *182* (1–3), 518–524.
23. Yantasee, W.; Warner, C. L.; Sangvanich, T.; Addleman, R. S.; Carter, T. G.; Wiacek, R. J.; Fryxell, G. E.; Timchalk, C.; Warner, M. G. *Environ. Sci. Technol.* **2007**, *41* (14), 5114–5119.
24. Lin, Y.; Chen, H.; Lin, K.; Chen, B.; Chiou, C. *J. Environ. Sci.* **2011**, *23* (1), 44–50.
25. Pearson, R. G. *J. Chem. Educ.* **1968**, *45* (9), 581.
26. Lin, T. L.; Lien, H. L. *Int. J. Mol. Sci.* **2013**, *14* (5), 9834–9847.
27. Nelson, D. L., Cox, M. M. *Lehninger Principles of Biochemistry*, Fifth Edit.; Katherine Ahr, Ed.; W. H. Freeman and Company: New York, 2008.
28. Wang, J.; Zheng, S.; Shao, Y.; Liu, J.; Xu, Z.; Zhu, D. *J. Colloid Interface Sci.* **2010**, *349* (1), 293–299.
29. Nuryono, N.; Rosiati, N.; Rusdiarso, B.; Sakti, S. C.; Tanaka, S. *Springerplus* **2014**, *3* (1), 515.
30. Amaria, A.; Suyono, S.; Sugiharto, E.; Rohmah, A. N. *Indones. J. Chem.* **2010**, *10* (2), 177–183.
31. Casillas, P. E. G.; Gonzalez, C. A. R.; Pérez, C. A. M. *Infrared Spectroscopy of Functionalized Magnetic Nanoparticles*; Theophile, T., Ed.; Intech: Rijeka, Croatia, 2012.
32. Silverstein, M. R.; Webster, F. X.; Kiemle, J. D. *Spectrometric Identification of Organic Compounds*, Seventh Ed.; Brennan, D., Ed.; John Wiley & Sons, Inc.: Hoboken United States of America, 2005.
33. Ahangaran, F.; Hassanzadeh, A.; Nouri, S. *Int. Nano Lett.* **2013**, *3*, 3–7.
34. Nuryono, N.; Muliaty, E.; Rusdiarso, B.; Candra, S.; Sakti, W.; Tanaka, S. *J. Ion Exch.* **2014**, *25* (4), 114–121.
35. Kumar, S.; Rai, S. B. *J. Pure Appl. Phys.* **2010**, *48* (April), 251–255.
36. Fajaroh, F.; Setyawan, H.; Nur, A.; Lenggoro, I. W. *Adv. Powder Technol.* **2013**, *24* (2), 507–511.
37. Nuryono, N.; Syukur, M.; Kuncaka, A.; Sakti, S. C. W. *Indones. J. Chem.* **2016**, *16* (2), 130–137.
38. Ursachi, I.; Vasile, A.; Chiriac, H.; Postolache, P.; Stancu, A. *Mater. Res. Bull.* **2011**, *46* (12), 2468–2473.
39. Wu, W.; He, Q.; Jiang, C. *Nanoscale Res. Lett.* **2008**, *3* (11), 397–415.
40. Roto, R.; Yusran, Y.; Kuncaka, A. *Appl. Surf. Sci.* **2016**, *377*, 30–36.
41. Persson, J.A., Wennerholm, M., OHalloran, S. *Handbook for*; FOSS, DK-3400 Hilleroed: Denmark, 2008.
42. Zhuravlev, L. T. *Colloids Surfaces A Physicochem. Eng. Asp.* **2000**, *173* (1–3), 1–38.
43. Shajesh, P.; Smitha, S.; Aravind, P. R.; Warrier, K. G. K. *J. Sol-Gel Sci. Technol.* **2009**, *50* (3), 353–358.
44. El-Naggar, A. Y. *J. Emerg. Trends Eng. Appl. Sci.* **2013**, *4* (1), 144–148.
45. Sun, Z. H.; Xu, D.; Wang, X. Q.; Zhang, G. H.; Yu, G.; Zhu, L. Y.; Fan, H. L. *Cryst. Res. Technol* **2007**, *42*, 812–816.
46. Si, S.; Kotal, A.; Mandal, T. K.; Giri, S.; Nakamura, H.; Kohara, T. *Chem. Mater* **2004**, *16* (11), 3489–3496.
47. Wang, Z.; Zhu, H.; Wang, X.; Yang, F.; Yang, X. *Nanotechnology* **2009**, *20* (46), 465606.
48. Kalska-Szostko, B.; Wykowska, U.; Satula, D.; Nordblad, P. *Beilstein J. Nanotechnol.* **2015**, *6*, 1385–1396.
49. Pac^{3}awski, K.; Fitzner, K. *Metall. Mater. Trans. B* **2004**, *35* (December), 1071–1085.
50. Buhani; Narsito; Nuryono; Kunarti, E. S. *Desalination* **2010**, *251* (1–3), 83–89.
51. Adamson W. A., Gast, P. A. *Physical Chemistry of Surface*, Sixth.; John Wiley & Sons: New York, 1997.
52. Gurung, M.; Adhikari, B. B.; Kawakita, H.; Ohto, K.; Inoue, K.; Alam, S. *Chem. Eng. J.* **2011**, *174* (2–3), 556–563.
53. Ho, Y. S.; Mckay, G. *Process Biochem.* **1999**, *34*, 451–465.
54. Ramesh, A.; Hasegawa, H.; Sugimoto, W.; Maki, T.; Ueda, K. *Bioresour. Technol.* **2008**, *99* (9), 3801–3809.
55. Liu, L.; Liu, S.; Zhang, Q.; Li, C.; Bao, C.; Liu, X.; Xiao, P. *J. Chem. Eng. Data* **2013**, *58* (2), 209–216.